Energetic Radiation Produced During Rocket-Triggered Lightning

Joseph R. Dwyer, *et al.*

Science **299**, 694 (2003);
DOI: 10.1126/science.1078940

Science (print ISSN 0036-8075; online ISSN 1095-9203) is published weekly, except the last week in December, by the American Association for the Advancement of Science, 1200 New York Avenue NW, Washington, DC 20005.

al clue as to why the tropical oceans exerted such strong control over atmospheric events leading to the droughts of 1998–2002. Together with the unusual persistence of the tropical-wide SST anomaly pattern itself, the modeling results offer compelling evidence that the widespread mid-latitude drought was strongly determined by the tropical oceans. It is thus more than figurative, although not definitive, to claim that this ocean was "perfect" for drought insofar as it satisfied many of the requirements for severe, sustained precipitation deficits and temperature increases.

To what, then, can the tropical SST anomalies of 1998–2002 be attributed? ENSO is a naturally occurring fluctuation of the coupled ocean-atmosphere system (*20*), and climate proxy records (for instance, ice cores, tree rings, and corals) suggest that this phenomenon has occurred for millennia (*21*). Even the persistence of the cold SST conditions during the 4-year period, although unusual, was not unprecedented (*10*, *22*). This and other evidence indicates that the recent statistics of ENSO have not changed detectably beyond the range of natural variability (*23, 24*). On the other hand, the warmth of the tropical Indian Ocean and the west Pacific Ocean was unsurpassed during the 20th century, being embedded within a multidecade warming trend. Climate attribution studies find that this warming (roughly 1°C since 1950) is beyond that expected of natural variability and is partly due to the ocean's response to increased greenhouse gases (*25, 26*). The state of the tropical ocean during 1998–2002 thus combined a naturally occurring, interannual cooling of the eastern Pacific with a lower frequency, possibly inexorable, warming of the Indian and west Pacific oceans. The resultant exaggeration of zonal contrast in SST did not occur during the prior, protracted La Niña periods of the 20th century, providing a unique oceanic condition during 1998–2002. It is an open question whether such tropical oceanic forcings will become more prevalent during the 21st century. Because of deficiencies in coupled ocean-atmosphere models, little confidence exists with regard to projections of the future statistics of ENSO (such as its duration and amplitude) or of the regional pattern of mean tropical SST change itself. The atmospheric modeling results of 1998–2002 suggest an increased risk for severe and synchronized drying of the mid-latitudes if the tropical mean SSTs or their interannual variability increase the ocean's west-east contrast over the equatorial Pacific.

References and Notes

1. G. Bell *et al.*, *Bull. Am. Meteorol. Soc.* **81**, 1328 (2000).
2. J. Lawrimore *et al.*, *Bull. Am. Meteorol. Soc.* **82**, 1304 (2001).
3. A. M. Waple *et al.*, *Bull. Am. Meteorol. Soc.* **83**, 938 (2002).
4. IPCC, *Climate Change 2001: The Scientific Basis: Summary for Policy Makers and Technical Summary of the Working Group I Report* (Cambridge Univ. Press, Cambridge, 2001).
5. IPCC, *Climate Change 2001: Impacts, Adaptation, and Vulnerability: Contributions of Working Group II to the Third Assessment of the IPCC* (Cambridge Univ. Press, Cambridge, 2001).
6. K. E. Trenberth et al., *J. Geophys. Res.* **103**, 14291 (1998).
7. C. F. Ropelewski, M. S. Halpert, *Mon. Weather Rev.* **115**, 1606 (1987).
8. _____, *J. Clim.* **2**, 268 (1989).
9. G. N. Kiladis, H. F. Diaz, *J. Clim.* **2**, 1069 (1989).
10. J. E. Cole, J. T. Overpeck, E. R. Cook, *Geophys. Res. Lett.*, in press.
11. M. Barlow, H. Cullen, B. Lyon, *J. Clim.* **15**, 697 (2002).
12. D. W. J. Thompson, J. M. Wallace, *Geophys. Res. Lett.* **25**, 1297 (1998).
13. G. Branstator, *J. Clim.* **15**, 1893 (2002).
14. The variability of 4-year–averaged, consecutive June–May periods was calculated based on monthly SSTs from 1948 to 1998. Fifty-one overlapping 4-year periods were used to calculate the standard deviation of 4-year averages, and this result was used to standardize the June 1998–May 2002 SST anomaly.
15. The model data are from a 24-member ensemble of the European Centre–Hamburg model (ECHAM4.5) run at the International Research Institute for Climate Prediction (IRI), an 18-member ensemble of the National Center for Environmental Predictions (NCEP) climate model, and a 9-member ensemble of the NASA Seasonal to Interannual Prediction Program (NSIPP) model. The configuration of the NCEP and ECHAM models uses triangular wavenumber 42 (T42) horizontal spectral resolution with 18 unequally spaced vertical (sigma) levels. The NSIPP model is a grid-point model with 2° horizontal resolution and 34 vertical levels. Observed, monthly SSTs are assigned to the mid-month date and are updated with linear interpolation for every time step at each ocean grid point. As of 2002, each of these model versions was being used by the three centers to make dynamical seasonal climate predictions.
16. Ensemble experiments are performed to detect the climate signal related to the imposed lower boundary forcing. In this approach, individual model realizations are begun from different atmospheric initial conditions, but each realization is subjected to identically evolving sea surface boundary conditions. The process of averaging the separate realizations extracts the recurrent atmospheric signal related to the boundary forcing and suppresses the random atmospheric fluctuations that are unrelated to that forcing.
17. M. Hoerling, A. Kumar, data not shown.
18. The experiments using an idealization of the 1998–2002 tropical SST forcing were performed with a recent version of the NCAR Community Climate Model known as CCM3. The standard model configuration is T42 horizontal spectral resolution with 18 unequally spaced vertical (hybrid) levels.
19. The spatial correlation of 200-mbar height anomalies poleward of 20°N between the GCM results forced by global SSTs and those calculated with the idealized 4-year–averaged tropical SSTs is 0.9.
20. S. G. Philander, *El Niño, La Niña, and the Southern Oscillation* (Academic Press, New York, 1990).
21. V. Markgraf, H. F. Diaz, in *El Niño and the Southern Oscillation: Multiscale Variability and Global and Regional Impacts,* H. F. Diaz, V. Margraf, Eds. (Cambridge Univ. Press, Cambridge, 2000), pp. 465–488.
22. At least three prior instances during the 20th century can be found in which La Niña conditions spanned three consecutive years, most notably 1908–1910, 1954–1957, and 1973–1975. Over the United States, the period 1954–1957 was a particularly severe drought period, whereas the other two protracted La Niña periods were not widespread droughts.
23. B. Rajagopalan, U. Lall, M. Cane, *J. Clim.* **10**, 2351 (1997).
24. A. Timmermann, *J. Atmos. Sci.* **56**, 2313 (1999).
25. T. R. Knutson, T. L. Delworth, K. W. Dixon, R. J. Stouffer, *J. Geophys. Res.* **104**, 30981 (1999).
26. T. R. Knutson, S. Manabe, *J. Clim.* **11**, 2273 (1998).

27. Supported by NOAA's Office of Global Programs Regional Integrated Sciences and Assessments Program, the Climate Variability/Pacific Program, and the Climate Dynamics and Experimental Predictions Program. We thank L. Goddard of the IRI and M. Suarez of NASA, who provided the ECHAM and NSIPP model data, respectively, and G. Bates and T. Y. Xu for assisting with model experiments and analysis.

3 October 2002; accepted 16 December 2002

Energetic Radiation Produced During Rocket-Triggered Lightning

Joseph R. Dwyer,[1]* Martin A. Uman,[2] Hamid K. Rassoul,[1] Maher Al-Dayeh,[1] Lee Caraway,[1] Jason Jerauld,[2] Vladimir A. Rakov,[2] Douglas M. Jordan,[2] Keith J. Rambo,[2] Vincent Corbin,[1] Brian Wright[1]

Using a NaI(Tl) scintillation detector designed to operate in electrically noisy environments, we observed intense bursts of energetic radiation (≫10 kiloelectron volts) during the dart leader phase of rocket-triggered lightning, just before and possibly at the very start of 31 out of the 37 return strokes measured. The bursts had typical durations of less than 100 microseconds and deposited many tens of megaelectron volts into the detector. These results provide strong evidence that the production of runaway electrons is an important process during lightning.

Attempts to measure x-ray emission from lightning have been intermittently reported since 1925, when C. T. R Wilson (*1*) first proposed that the strong electric fields associated with thunderstorms could accelerate electrons to relativistic energies. However, these results have been generally inconclusive because of the sporadic nature of lightning and the electromagnet-

ically noisy environment it generates (*2*). In this report, we present observations of energetic radiation produced in association with rocket-triggered lightning. These results have important implications not only for lightning physics but also for the fundamental process of the runaway breakdown of air, in which electrons are accelerated to relativistic energies by strong electric fields (*3*).

Rocket-triggered lightning is a useful tool for studying lightning processes, allowing both the time and the location of lightning strikes to be controlled. Lightning discharges to the ground are complicated but can loosely be divided into two phases: the leader phase, in which channels of ionization are created between the cloud and the ground, and the return stroke phase, in which a large current flows, starting at the ground and propagating upward, draining the charge from the leader channel. The leader phase is of particular interest for runaway breakdown because large electric fields can be generated in front of the downward-propagating leaders. There are two basic types of leaders associated with cloud-to-ground lightning: the stepped leaders, which take a halting, tortuous path from the cloud to the ground, and the faster dart leaders, which follow a more direct path. Most triggered lightning strokes produce only dart leaders and are similar to the subsequent strokes in natural lightning. Preliminary observations indicate that stepped leaders may produce energetic radiation in natural lightning (*4*), but no such measurements have been reported for dart leaders or for triggered lightning.

The characteristic signals from the instrument used for the energetic radiation measurements (*5*) are illustrated in Fig. 1, which shows the preamplifier output signals from the active NaI(Tl)/photomultiplier tube (PMT) detector and the control PMT detector (without scintillator), produced by a single 662-keV gamma ray from a radioactive source. The detector response function, determined by the preamplifier circuit, is plotted as a black dashed line in Fig. 1 and allows signals from energetic particles to be distinguished from spurious signals.

On 20 July, 25 July, and 13 September 2002, a total of seven rocket-triggered lightning flashes were produced during thunderstorm conditions at the International Center for Lightning Research and Testing at Camp Blanding, Florida (*5*). These flashes contained a total of 37 leader/return stroke sequences that terminated at the rocket launcher. Intense bursts of energetic radiation were observed just before 84% of these return strokes. The observations are consistent with most of the energetic radiation occurring during the dart leader phase, although some additional contribution from the start of the return strokes cannot be ruled out. The term "energetic radiation" is used here, because the detector cannot distinguish between x-rays/gamma rays and energetic electrons. Because of the attenuation of x-rays/gamma rays and energetic electrons in the atmosphere, this observed energetic radiation almost certainly originated within a few hundred meters of the instrument and, therefore, was most likely produced by the local electric fields associated with the lightning and not by electric fields in the overhead thunderclouds.

Figure 2, which shows the data for the first stroke of the third flash on 20 July, has an energetic radiation signal beginning just before the return stroke, the time of which (derived from the current measurement at the launch tower) is indicated by the vertical dotted line. No such signal is present from the control detector, which is consistent with energetic radiation. The black dashed line shows the detector response function for an energetic particle detected at the time of the return stroke. The only free parameter in the fit of the response function to the data is the signal amplitude. As Fig. 2 illustrates, the pulse shape is consistent with that of energetic radiation with a deposited energy of ~3 MeV. Indeed, the 45-μs decay time seen in the data indicates that charge was deposited in the front end of the preamplifier, which cannot be explained by noise pickup in the system.

Because for each lightning flash an entire 1 s of data was recorded, followed by another 1-second background record, about 10 s later, the background rate as a function of energy was accurately measured and found to be 23 counts/s for pulse heights above 0.5 V, corresponding to energies above 1.5 MeV. Based on these measurements, the odds that a background signal produced this event are calculated to be much less than 1 in 4300.

Figure 3 shows the output signals associated with the second leader/return stroke sequence of the second flash on 20 July 2002. The energetic radiation signature seen in the active detector is

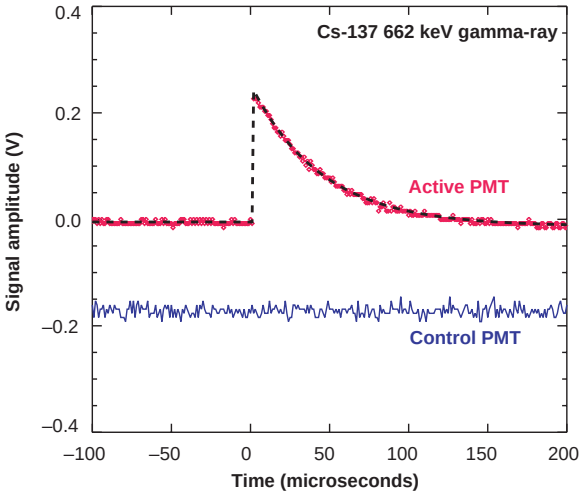

Fig. 1. Output signals from the active PMT (top red data points) and control PMT (bottom blue line) for one 662-keV gamma ray emitted by a Cs-137 radioactive source. The control data have been shifted down for clarity. The black dashed line is the detector response function calculated from the preamplifier circuit.

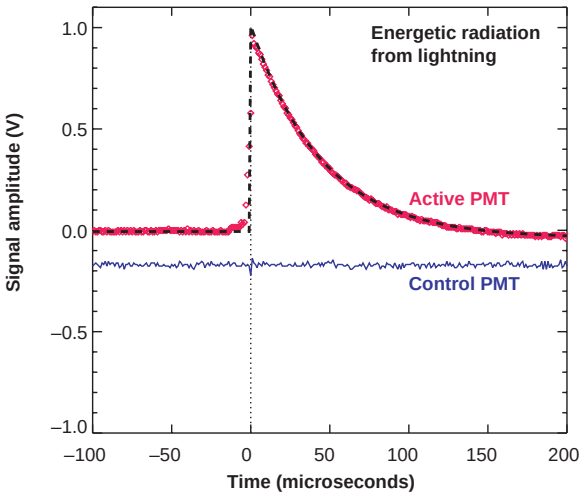

Fig. 2. Output signals from the active PMT (top red data points) and control PMT (bottom blue line) measured in association with a triggered lightning leader/return stroke sequence. The control data have been shifted down for clarity. The vertical dotted line shows the time of the return stroke determined by the current measured at the launch tower. The black dashed line is the detector response function, corresponding to an energetic particle depositing 3 MeV in the NaI(Tl) at the time of the return stroke. The rise time from the active PMT can be seen to be considerably slower than the 100-ns rise time produced by a single energetic particle (black dashed line), indicating that this event is produced by more than one high-energy photon or electron, with energetic particles arriving between 0 and 16 μs before the return stroke.

[1]Department of Physics and Space Sciences, Florida Institute of Technology, Melbourne, FL 32901, USA. [2]Department of Electrical and Computer Engineering, University of Florida, Gainesville, FL 32611, USA.

*To whom correspondence should be addressed.

much larger than that shown in Fig. 2 and, in fact, is clipped at 1 V, at the maximum value of the analog-to-digital converter (ADC) in the data acquisition card. Nevertheless, the trailing edge of the signal can still be fit to the detector response function (black dashed line in Fig. 3) and is again completely consistent with energetic radiation, this time with a total deposited energy of ≫10 MeV.

Although the active detector produced a very large signal for this event, the control detector produced only a very small response. The signal from the control has a pulse shape consistent with the detector response function (i.e., a 45-μs decay) but with the very small amplitude of ~0.02 V. The gain on the control detector's fiber optic receiver is actually 4.2 times larger than for the active detector, making the contrast between the sizes of the signals from the two detectors even larger. The small signal from the control detector may have been produced by energetic radiation directly striking the PMT photocathode. Similar small signals have been observed from the control PMT using a Co-60 gamma-ray source. The return stroke occurred at time zero in the figure and can be seen in the lower two panels of Fig. 3, which plot the electric current measured at the launch tower and the change in the vertical electric field, measured by a 0.16-m^2 flat-plate antenna 260 m away. The energetic radiation precedes the return stroke by 160 μs (Fig. 3), a time period corresponding to the dart leader phase of the lightning. A photograph of the triggered lightning flash that produced the data in Fig. 3 is shown in Fig. 4.

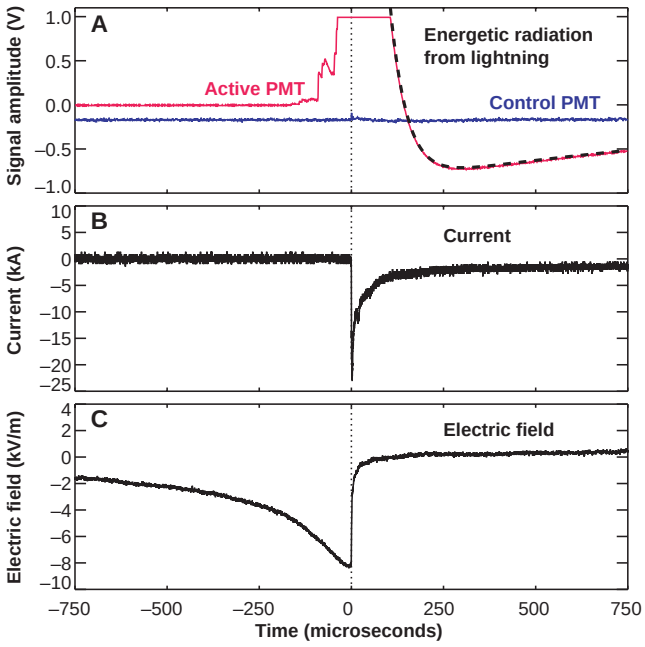

Fig. 3. (**A**) Output signals from the active PMT (red line) and control PMT (blue line) measured in association with a triggered lightning leader/return stroke sequence. This event is clipped at 1 V because of saturation of the ADC. The black dashed line shows the detector response for an impulse of ~80 MeV of total deposited energy in the NaI(Tl) 10 μs before the return stroke (vertical dotted line). The energetic particle signal begins 160 μs before the return stroke, and the sawtooth pattern that occurred during the rise phase indicates that several distinct energetic particle events occurred before the return stroke. (**B**) Current associated with the lightning return stroke measured at the launch tower. The current provides the external trigger (threshold = –7.1 kA) for the data acquisition electronics. (**C**) Vertical electric field measured 260 m from the launch tower. The electric field before zero time is a result of a downward-propagating negatively charged dart leader. The field after zero is the result of an upward-propagating return stroke discharging the leader channel.

Fig. 4. Still photograph of the second triggered lightning flash on 20 July 2002. The exposure was for 6 s and contains all strokes for this flash (the narrow and twisting channels). The wider central column is from the burning of the copper wire that trailed from the rocket; that burning was due to the initial stage current that precedes the leader and return stroke sequences. The structure at the bottom of the picture is the top of the launch tower. The return strokes terminate on a rod attached to the launch tubes.

Because of their high intensity and short duration, the events reported here cannot be explained by variations in the naturally occurring background rate, such as from radioactive washout (*6*) or variations in the cosmic ray rate from meteorological effects (*7*). Based on background measurements made by the instrument, the odds that the event seen in Fig. 3 is an accidental coincidence with a naturally occurring background event, such as an atmospheric cosmic ray, are calculated to be much less than 1 in 3750.

The large saturating signal with a complicated rise before the return stroke, shown in Fig. 3, is typical of the 21 energetic radiation events observed on 20 and 25 July 2002. Of these events, only two had peaks below 1 V. On the other hand, for the 10 events observed on 13 September 2002, the majority were similar to the event shown in Fig. 2, with peaks below 1 V. The smaller signal sizes seen on 13 September may be explained by the distance between the instrument and the launcher; in September, the instrument was twice as far from the launcher as it was in July.

All the energetic radiation events, regardless of size, have signals with exponential decays that are completely consistent with the detector response. Furthermore, unlike gamma rays from radioactive sources and unlike cosmic ray events, all the energetic radiation events observed in association with lightning have complicated rising portions, indicating that multiple energetic particles (x-rays, gamma rays, or energetic electrons) are producing the signals. The attenuation of x-rays in the 0.32-cm aluminum window on the top of the instrument increases rapidly below about 30 keV, with 30-keV x-rays attenuated to 0.42 times their original number

and 10-keV x-rays attenuated to 3.6×10^{-8} times their original number, making it unlikely that the instrument is measuring x-rays below 10 keV.

Our results are similar to those of Moore *et al.* (*4*), who observed energetic radiation from natural lightning in association with the stepped leader phase. The radiation seen by Moore *et al*. occurred for several milliseconds before the return stroke, whereas we observed energetic radiation up to 160 μs before the return stroke. Because stepped leaders are usually not produced during the traditional form of rocket-triggered lightning used for our study, the difference in the time scales between the two observations may reflect the fact that the average speed of dart leaders is about one to two orders of magnitude faster than that of stepped leaders.

When taken together with observations of x-ray bursts in thunderstorms (*8*–*12*) and terrestrial gamma-ray bursts (*13*–*15*), these new observations indicate that runaway electrons are commonly produced in atmospheric discharges. Furthermore, because triggered lightning can make copious amounts of energetic radiation, such experiments make the detailed study of this phenomenon practical.

References and Notes

1. C. T. R. Wilson, *Proc. Camb. Philos. Soc.* **22**, 534 (1925).
2. D. M. Suszcynsky, R. Roussel-Dupre, G. Shaw, *J. Geophys. Res.* **101**, 23505 (1996).
3. A. V. Gurevich, G. M. Milikh, R. Roussel-Dupre, *Phys. Lett. Ser. A* **165**, 463 (1992).
4. C. B. Moore, K. B. Eack, G. D. Aulich, W. Rison, *Geophys. Res. Lett.* **28**, 2141 (2001).
5. Materials and methods are available as supporting material on *Science* Online.
6. R. S. Foote, in *Natural Radiation Environment*, J. A. S. Adams, W. M. Lowder, Eds. (Univ. of Chicago Press, Chicago, 1964), pp. 757–766.
7. J. Clay, E. M. Bruins, *Rev. Mod. Phys.* **11**, 158 (1939).
8. G. K. Parks, B. H. Mauk, R. Spiger, J. Chin, *Geophys. Res. Lett.* **8**, 1176 (1981).
9. M. McCarthy, G. K. Parks, *Geophys. Res. Lett.* **12**, 393 (1985).
10. K. B. Eack, W. H. Beasley, W. D. Rust, T. C. Marshall, M. Stolzenburg, *Geophys. Res. Lett.* **23**, 2915 (1996).
11. _____, *J. Geophys. Res.* **101**, 29637 (1996).
12. K. B. Eack, D. M. Suszcynsky, W. H. Beasley, R. Roussel-Dupre, E. Symbalisty, *Geophys. Res. Lett.* **27**, 185 (2000).
13. G. J. Fishman *et al*., *Science* **264**, 1313 (1994).
14. R. J. Nemiroff, J. T. Bonnell, J. P. Norris, *J. Geophys. Res.* **102**, 9659 (1997).
15. H. Feng, T. P. Li, M. Wu, M. Zha, Q. Q. Zhu, *Geophys. Res. Lett.* **29**, 6-1 (2002).

16. We thank those at Florida Tech who assisted in the construction of the instrument and the collection of the energetic radiation data. In particular, we thank I. Vodopianov for his assistance with the fiber optic cables. We also thank members of the University of Florida Lightning Research Laboratory for their work in producing triggered lightning at Camp Blanding. Supported in part by NSF (CAREER grant ATM 0133773 and grant ATM 0003994) and the Department of Transportation (Federal Aviation Administration) (grant 99-G-043).

Supporting Online Material

www.sciencemag.org/cgi/content/full/299/5607/694/DC1
SOM Text
References

1 October 2002; accepted 5 December 2002

Paucity of Genes on the *Drosophila* X Chromosome Showing Male-Biased Expression

Michael Parisi,[1] Rachel Nuttall,[2] Daniel Naiman,[3] Gerard Bouffard,[4] James Malley,[5] Justen Andrews,[1]* Scott Eastman,[2]† Brian Oliver[1]‡

Sex chromosomes are primary determinants of sexual dimorphism in many organisms. These chromosomes are thought to arise via the divergence of an ancestral autosome pair and are almost certainly influenced by differing selection in males and females. Exploring how sex chromosomes differ from autosomes is highly amenable to genomic analysis. We examined global gene expression in *Drosophila melanogaster* and report a dramatic underrepresentation of X-chromosome genes showing high relative expression in males. Using comparative genomics, we find that these same X-chromosome genes are exceptionally poorly conserved in the mosquito *Anopheles gambiae*. These data indicate that the X chromosome is a disfavored location for genes selectively expressed in males.

The *Drosophila melanogaster* X chromosome is present in one dose in males and two in females. There are at least three aspects of this fact that might influence X-chromosome development over large time scales. First, the dose difference has led to a dosage-compensation mechanism based on elevated transcription of X-chromosome genes in males (*1*). However, some X-chromosome genes may be expressed at lower levels in males than females because of dose, especially in germ cells where dosage compensation has not been documented (*2*). This might be a disadvantageous condition for genes encoding abundant male-specific proteins. Second, as males are hemizygous, mutations in X-chromosome genes are immediately available for selection even if those mutations would be recessive in diploids (*3*, *4*). This would promote accumulation of genes with functions favorable to males on the X chromosome. Third, two-thirds of the X chromosomes in a population reside in females. Positive selection in females would lead to X feminization, whereas selection against male-advantage genes deleterious to females would lead to demasculinization of the X chromosome.

Genes showing sex-biased gene expression profiles are also likely to have sex-biased functions. To investigate how genes with sex-differential expression profiles are distributed among the chromosomes in *Drosophila*, we have used an Incyte microarray to assay the expression of 14,142 predicted transcripts in competitive hybridizations [available from the Gene Expression Omnibus (*5*) under accessions GPL20, and GSM2456-GSM2469]. Sex-bias is conservatively defined as greater than twofold and is justified by the observation that >99% of array elements are within twofold in control hybridizations (Fig. 1A). Recent work has shown that sex-biased gene expression is significant in *Drosophila* (*6*–*8*). This first report of sex-biased expression of the full (predicted) genome also strongly indicates that there is significant sex-biased expression—especially in gonads (Fig. 1, B to D).

To investigate how genes with sex-biased expression are distributed in the genome, we parsed the data according to chromosome location (Fig. 2). The X chromosome showed a significant departure from a random distribution of genes with male-biased expression. For example, in gonad (Fig. 2A), only 10% of the transcripts were male-biased (at a twofold cutoff), whereas 14 to 17% of the autosomal transcripts showed male-biased differential expression. This highly significant underrepresentation of X-chromosome genes with male-biased expression held at 4- and 10-fold cutoffs as well (Fig. 2A). Similarly, with no cutoff, 45% of X-chromosome genes were expressed preferentially in testis. Corresponding frequencies for the autosome arms were 57, 57, 58, and 56%. We also examined the expression profiles of whole male flies and male flies with gonads removed (Fig. 2, D and G). Although the number of genes showing male-biased expression is

[1]Laboratory of Cellular and Developmental Biology, National Institute of Diabetes and Digestive and Kidney Diseases, National Institutes of Health, Department of Health and Human Services, Bethesda, MD 20892–8028, USA. [2]Incyte Genomics, Palo Alto, CA 94304, USA. [3]Department of Mathematical Sciences, Johns Hopkins University, Baltimore, MD 21218, USA. [4]National Institutes of Health Intramural Sequencing Center, National Human Genome Research Institute, National Institutes of Health, Department of Health and Human Services, Gaithersburg, MD 20877, USA. [5]Center for Information Technology, National Institutes of Health, Department of Health and Human Services, Bethesda, MD 20892–5620, USA.

*Present address: Center for Genomics and Bioinformatics, Indiana University, Bloomington, IN 47405–3700, USA.
†Present address: Quantum Dot Corporation, Hayward, CA 94545, USA.
‡To whom correspondence should be addressed. E-mail: oliver@helix.nih.gov